An Old Kinetic Method for a New Polymerization Mechanism: Toward Photochemically Mediated ATRP

Yin-Ning Zhou and Zheng-Hong Luo
Dept. of Chemical Engineering, School of Chemistry and Chemical Engineering, Shanghai Jiao Tong University, Shanghai 200240, P.R. China

DOI 10.1002/aic.14792
Published online March 29, 2015 in Wiley Online Library (wileyonlinelibrary.com)

With the idea of "an old method for a new mechanism," a detailed kinetic insight into photochemically mediated atom-transfer radical polymerization (photo ATRP) was presented through a validated comprehensive model. The simulation mimics the experimental results of the model system using optimized photochemically mediated radical generation rate coefficients. The activator and radical (re)generated from the photo mediated reactions endow the photo ATRP with unique features, such as rapid ATRP equilibrium and quick consumption of initiator with a small amount of residual. The effect of the reaction parameters on ATRP behaviors was also investigated. Results showed that the acceleration of polymerization rate follows the square root law in the following three cases: the overall photochemically mediated radical generation rate coefficients (k_r), the free ligand concentration, and the initiator concentration. However, the independence of the apparent propagation rate coefficient (k_p^{app}) on the square root of catalyst concentration might be attributed to the result of the synergy between the activators regenerated by electron-transfer ATRP and the initiators for continuous activator regeneration ATRP mechanism. The photo ATRP is able to design and prepare various polymers by carefully tuning the conditions using the model-based optimization approach.
 AIChE J*, 61: 1947–1958, 2015*
Keywords: photochemically mediated ATRP, kinetic model, parameter estimation, model-based optimization

Introduction

The increasing demand of polymer production in our society has led to significant development in macromolecular reaction engineering.[1] As a branch of chemical reaction engineering that plays an important function in various industrial fields, macromolecular reaction engineering follows similar principles to produce and process the polymeric materials. Specifically, three major questions need to be answered: "How far?," "How fast?," and "How to?"[1,2] For each specific reaction, the first question is commonly based on a clarified reaction mechanism and can be answered by thermodynamics. Subsequently, kinetic studies are carried out to answer the second question. Using a well-built kinetic model with proper kinetic rate coefficients, one can design and operate reactor systems, and discriminate the reaction mechanisms including new, pendent, or controversial mechanism. Finally, the model-based optimization of reaction conditions and the choice of reactor can determine how a structurally well-defined and cost-effective product is prepared.[2] The aforementioned core knowledge indicates that kinetic investigation remains an important issue in the chemical reaction engineering field, although it is an old method.[3]

The development of the chemistry field has led to the emergence of numerous new experimental and analytical methods that help scientists to discover new chemical reactions. An example of a research focused on macromolecular chemistry is the reversible deactivation radical polymerization (RDRP) techniques, which have been studied since their discovery a couple of decades ago.[4,5] Among these techniques, atom-transfer radical polymerization (ATRP) has been researched extensively because of their brilliant ability in preparing polymers with well-defined and complex architectures.[6–8] However, the industrialization of ATRP technique still has a long way to go, which includes mechanism and kinetics study, although a few achievements have already been made.[9] In ATRP, the use of low oxidation state transition-metal catalyst (commonly Cu^I salt) inevitably leads to contamination of products and time-consuming deoxygenation process.[9–11] Scientists have been focusing on diminishing the catalyst dosage and applying high oxidation state catalytic complex or metallic copper through experimental and kinetic modeling investigations.[12–26] For example, initiators for continuous activator regeneration (ICAR) ATRP,[13–16] activators regenerated by electron transfer (ARGET) ATRP,[17–19] single electron transfer-living radical polymerization (SET-LRP),[20–22] supplemental activator and reducing agent (SARA) ATRP,[23–25] and electrochemically mediated ATRP (eATRP)[26] have been investigated. Previous studies have indicated that well-constructed mathematical models are useful for kinetics studies, and can be applied to simulation,[15,19,22] optimization,[15,22] parameter estimation,[16] control,[19] and mechanistic investigation[24,25] of polymerization processes.

Additional Supporting Information may be found in the online version of this article.

Correspondence concerning this article should be addressed to Z. H. Luo at luozh@sjtu.edu.cn.

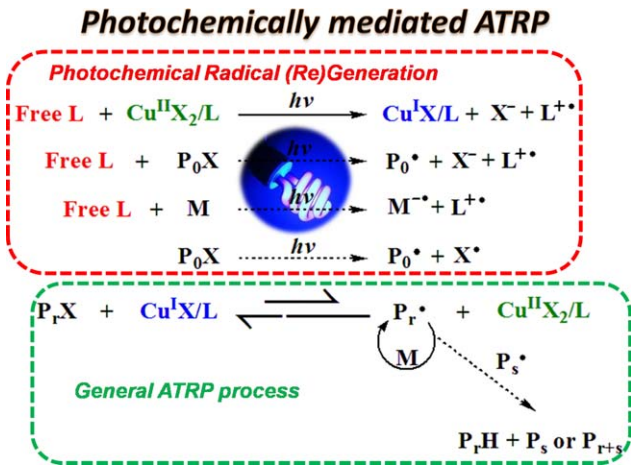

Scheme 1. The proposed mechanism of the photochemically mediated ATRP.

[Color figure can be viewed in the online issue, which is available at wileyonlinelibrary.com.]

Photo ATRP have attracted significant attention because of its facile operation and minimal addition of catalyst.[27–52] Among the non-copper photo ATRP techniques, Hawker et al. developed an efficient and facile technique for polymerization of methyl methacrylate (MMA) and a series of acrylate monomer using an Ir-based photoredox catalyst.[31,32] More recently, an important development of light-induced living polymerization was presented almost simultaneously by Hawker and coworkers and Miyake et al., which realized a metal-free ATRP with an organic visible-light photocatalyst.[36,37] In traditional Cu-mediated ATRP, Guan and Smart discovered that the rate and livingness of ATRP can be significantly improved under visible light irradiation.[39] Yagci and coworkers reported UV light-induced ATRP of MMA through directly reduction of $Cu^{II}X_2$/L to Cu^{I}X/L complex.[41] In addition, polymerization was enhanced by using methanol as solvent, causing the reaction to proceed in a homogeneous system.[42] Mosnáček and Ilčíková carried out UV light-mediated ATRP in a system with low Cu catalyst.[44] Subsequently, Matyjaszewski and coworkers investigated the effect of light sources on photoinduced ATRP by applying blue, violet LEDs, or even sunlight.[45] At that time, the mechanism held in these works were subject to a hybrid system of ICAR ATRP and ARGET ATRP in the presence of a stoichiometric ligand.[41–45] However, detailed investigations published by Haddleton and Matyjaszewski showed that a well-controlled polymerization should be carried out in a system with excess ligand, and the light-induced ATRP is an ARGET-dominated system with limited contribution from the ICAR mechanism.[46–49] Overall, with the merit of light in the temporal and spatial control of polymerization, photo ATRP has attracted increasing interest and has been used to synthesize the multiple-block copolymers and surface micropatterns.[50–52] However, no detailed kinetic study for this mechanism based on a well-built model has been conducted.

According to the above descriptions, kinetics and its modeling are old topics in chemical engineering, but remain a core issue in polymerization engineering. Furthermore, photochemically mediated ATRP with newly clarified reaction mechanism needs a thorough investigation for its application. Accordingly, with the idea of "an old method for a new mechanism," a comprehensive kinetic model of photo ATRP was developed in this work for the first time using the method of moments. The proposed photo ATRP mechanism is illustrated in Scheme 1. The presented model was validated by experimental data, and then used as a convenient and powerful tool to estimate the rate coefficients of photochemically radical (re)generation reactions based on methyl acrylate (MA) model system, which was carried out in dimethyl sulfoxide (DMSO) at 25°C. A kinetic simulation, as a supplement to the experiments, described the detailed information of all the species and reactions during the polymerization. Finally, the effects of reaction conditions, including the strength of light-induced reactions and the concentrations of free ligand, catalyst, and initiator on the kinetic behavior of photo ATRP were determined to understand and optimize the reaction process.

Kinetic Model and Computational Method

According to the proposed mechanism, all the relevant reactions and original rate coefficients are listed in Table 1. In the case of this specific system, the radicals generated from photochemical reactions include several parallel pathways, such as the reduction of $Cu^{II}X_2$/L deactivator ($Cu^{II}X_2 = CuBr_2$, L = Me_6TREN) in the presence of excess ligand (free L), the photochemical SET reaction between either an alkyl halide initiator [P_0X = ethyl 2-bromoisobutyrate (Eib-Br)] or a macroinitiator (P_rX = PMA-Br) with excess ligand, the unimolecular P_0X photochemical homolytic cleavage of the carbon-halogen bond, or the photochemical SET between excess ligand and monomer. In these processes, excess ligand acts as an electron donor. In general ATRP process, initiation, propagation, activation–deactivation equilibrium, chain transfer to ligand or initiator, and termination were considered in the kinetic model. However, chain transfer to the monomer, solvent, and polymer that led to branch formation was neglected under the present polymerization conditions.[20,24,25] Aside from the conventional radical termination, the reaction of Cu^{I}X/L mediated radical loss for secondary radicals was previously confirmed as the reason for the additional end functionality loss, and was thus taken into account.[56] Although the small radicals (re)generated from the photochemical and transfer reactions were essentially different, they are assumed to have similar reactivity in this work to simplify the simulations. It should be noted that an updated new propagation rate coefficient of MA (1.30×10^4 M^{-1} s^{-1} at 298 K) estimated by Barner-Kowollik et al.[59] is lower than that used in this work (1.56×10^4 M^{-1} s^{-1} at 298 K), which will slow down the overall rate of polymerization. However, to compare our simulation results with previous work reported by Ribelli et al.,[48] the used value of k_p was the same as that in Ribelli et al.'s work.

Molar balance equations for all species in the reactions can be established, as listed in Table 2. $P_r^{\cdot}(\mu)$, $P_rX(\lambda)$, and $P_r(\tau)$ denote the propagating radical chain, dormant chain, and dead chain species with the length of chain (r), respectively.

The numerical analysis of the kinetic equations listed in Table 2 can be easily conducted on a well-developed approach, that is, the method of moments. This method is a classical one that is suitable for kinetic study of the radical polymerization processes, as published in previous works by Zhu, D'Hooge, and our group.[1,18,25,60–68] The methodology is implemented by defining the moments for the chain

Table 1. Reactions for Photochemical ATRP Used in Simulation

Type of Reaction	Scheme	Rate Coefficient at 298 K[a]	Reference
Photochemical radical (re)generation[b]	$Cu^{II}X_2/L+L \xrightarrow{k_{r,C-L}} Cu^{I}X/L+L^{+\cdot}+X^-$	1.0×10^{-3}	48
	$P_0X+L \xrightarrow{k_{r,I-L}} P_0^{\cdot}+L^{+\cdot}+X^-$	6.2×10^{-6}	48
	$P_rX+L \xrightarrow{k_{r,MI-L}} P_r^{\cdot}+L^{+\cdot}+X^-$	1.4×10^{-6}[c]	48
	$P_0X \xrightarrow{k_{r,I}} P_0^{\cdot}+X^{\cdot}$	2.9×10^{-9}	48
	$L+M \xrightarrow{k_{r,L-M}} L^{+\cdot}+M^{-\cdot}$	1.5×10^{-9}	48
Initiation	$P_0X+Cu^{I}X/L \underset{k_{d0}}{\overset{k_{a0}}{\rightleftharpoons}} P_r^{\cdot}+Cu^{II}X_2/L$	2.0×10^{3} 5.0×10^{7}	24,53
	$P_0^{\cdot}+M \xrightarrow{k_{in}} P_1^{\cdot}$	7.3×10^{2}	54,55
Propagation	$P_r^{\cdot}+M \xrightarrow{k_p} P_{r+1}^{\cdot}$	1.56×10^{4}	54
ATRP equilibrium	$P_rX+Cu^{I}X/L \underset{k_{d0}}{\overset{k_{a0}}{\rightleftharpoons}} P_r^{\cdot}+Cu^{II}X_2/L$	2.0×10^{2} 2.8×10^{8}	24
Transfer	$P_r^{\cdot}+L \xrightarrow{k_{tr,L}} P_r+L^{\cdot}$	2.8×10^{3}	48
	$P_r^{\cdot}+P_0X \xrightarrow{k_{tr,I}} P_r+P_0X^{\cdot}$	2.3×10^{2}	48
Conventional radical termination[d]	$P_0^{\cdot}+P_0^{\cdot} \xrightarrow{k_{t0}} P_0P_0$	2.0×10^{9}	58
	$P_r^{\cdot}+P_0^{\cdot} \xrightarrow{k_{tr}} P_rP_0$	2.0×10^{9}	58
	$P_r^{\cdot}+P_s^{\cdot} \xrightarrow{k_t=k_{td}+k_{tc}} P_rH+P_s^{=}$ or P_{r+s}	1.0×10^{8}	58
Catalytic radical termination	$P_r^{\cdot} \xrightarrow[Cu^{I}X/L]{k_{t,C}} P_rH$ or $P_r^{=}$	4.0×10^{3}	48

[a]The units for all rate coefficients are $M^{-1}\ s^{-1}$, except that of $k_{r,I}$ is expressed in s^{-1}.
[b]The rate coefficients of photochemical radical (re)generation were also estimated in this work for comparing with those from Ref. 48.
[c]In the case of MA system, because secondary PMA-Br chain end closely resembles methyl 2-bromopropionate (MBP), $k_{r,MI-L}$ of PMA-Br uses the $k_{r,I-L}$ of MBP by analogy.[48]
[d]k_{tc} and k_{td} represent the combination and disproportionation termination rate coefficients with the values of $0.9k_t$ and $0.1k_t$, respectively.[56,57]

species first, and then a set of moment equations can be obtained accordingly. Detailed information is provided in Supporting Information Tables S1 and S2. By calculating the model equations in MATLAB 2012b (8.0), the concentrations of all reaction species, reaction rates, and a series of polymerization properties can be obtained as follows:

Reaction rates

$$R_{red,CL}=k_{r,C-L}\left[Cu^{II}X_2/L\right][L] \quad (1)$$

$$R_{red,IL}=k_{r,I-L}[P_0X][L] \quad (2)$$

$$R_{red,MIL}=k_{r,MI-L}[P_rX][L] \quad (3)$$

$$R_{red,I}=k_{r,I}[P_0X] \quad (4)$$

$$R_{red,LM}=k_{r,L-M}[P_0X][L] \quad (5)$$

$$R_p=k_p[M]\left[P_r^{\cdot}\right] \quad (6)$$

$$R_a=k_a\left[Cu^{I}X/L\right][P_rX] \quad (7)$$

$$R_d=k_d\left[Cu^{II}X_2/L\right]\left[P_r^{\cdot}\right] \quad (8)$$

$$R_{tr}=k_{tr,L}\left[P_r^{\cdot}\right][L]+k_{tr,I}\left[P_r^{\cdot}\right][P_0X] \quad (9)$$

$$R_t=k_{t0}\left[P_0^{\cdot}\right]\left[P_0^{\cdot}\right]+k_{tR}\left[P_r^{\cdot}\right]\left[P_0^{\cdot}\right]+k_t\left[P_r^{\cdot}\right]\left[P_s^{\cdot}\right]+k_{t,C}\left[P_r^{\cdot}\right]\left[Cu^{I}X/L\right] \quad (10)$$

Number-average molecular weight (M_n)

$$M_n=\overline{M}_{monomer}\frac{\sum\left(\lambda^1+\mu^1+\tau^1\right)}{\sum\left(\lambda^0+\mu^0+\tau^0\right)} \quad (11)$$

Weight-average molecular chain length (M_w)

$$M_w=\overline{M}_{monomer}\frac{\sum\left(\lambda^2+\mu^2+\tau^2\right)}{\sum\left(\lambda^1+\mu^1+\tau^1\right)} \quad (12)$$

Molecular weight distribution (M_w/M_n)

$$M_w/M_n=\frac{\sum\left(\lambda^2+\mu^2+\tau^2\right)}{\sum\left(\lambda^0+\mu^0+\tau^0\right)} \quad (13)$$

Chain-end functionality (F_t)

$$F_t=\frac{\left[\lambda^0\right]}{[P_0X]+\left[P_0^{\cdot}\right]_{r,C-L}+\left[P_0^{\cdot}\right]_{r,L-M}+\left[P_0^{\cdot}\right]_{tr,L}} \quad (14)$$

Results and Discussion

Simulation of photochemically mediated ATRP

The experimental data (black circle) were obtained from the work as reported by Ribelli et al.[48] under the following conditions: $[MA]_0:[Eib\text{-}Br]_0:[CuBr_2]:[Me_6TREN]_0 = 300:1:0.03:0.18$, [MA] = 7.4 M, MA/DMSO = 2/1 (v/v), with 392-nm UV light irradiation and at 25°C. The simulations were first conducted at the identical conditions, which can be compared with the results presented in Ribelli's work. Using the original rate coefficients listed in Table 1, the simulation results in Figure 1 (blue dash lines) shows slower polymerization rate and lower conversion than the experimental data within 25,000 s. The conversion of MA reached 98% when the simulation time was prolonged to 80,000 s, as shown in Supporting Information Figure S1. The evolution trends of the polymerization outcomes (i.e., $\ln([M]_0/[M]_t)$, M_n, M_w/M_n, and F_t) are similar to those in previous work,[48] which imply the reliability of the model developed in this study.

A linear semilogarithmic kinetic plot is expected to be observed in a well-controlled ATRP system, which indicates

Table 2. Kinetic Equations for All Species in Photochemical ATRP

Type	Mass Balance Equations
Macromolecules	
Propagating radical chains	$\frac{d[P_r^{\cdot}]}{dt}=k_p[P_{r-1}^{\cdot}][M]-k_p[P_r^{\cdot}][M]+k_a[P_rX]\left[Cu^IX\right]-k_d[P_r^{\cdot}]\left[Cu^{II}X_2\right]+k_{r,MI\text{-}L}[P_rX][L]-k_{tr,\ L}[P_r^{\cdot}][L]-k_{tr,\ I}[P_r^{\cdot}][P_0X]-k_{tR}[P_r^{\cdot}][P_0^{\cdot}]-\sum_{s=1}^{\infty}(k_{tc}+k_{td})[P_r^{\cdot}][P_s^{\cdot}]-k_{t,\ C}[P_r^{\cdot}]\left[Cu^IX\right]$
Dormant chains	$\frac{d[P_rX]}{dt}=k_d[P_r^{\cdot}][Cu^{II}X_2]-k_a[P_rX][Cu^IX]-k_{r,MI\text{-}L}[P_rX][L]$
Dead chains	$\frac{d[P_r]}{dt}=k_{tr,\ L}[P_r^{\cdot}][L]+k_{tr,\ I}[P_r^{\cdot}][P_0X]+k_{tR}[P_r^{\cdot}][P_0^{\cdot}]+\sum_{s=1}^{\infty}k_{td}[P_r^{\cdot}][P_s^{\cdot}]+\frac{1}{2}\sum_{s=1}^{r}k_{tc}[P_s^{\cdot}][P_{r-s}^{\cdot}]+k_{t,\ C}[P_r^{\cdot}]\left[Cu^IX\right]$
Small molecules	
Monomer	$\frac{d[M]}{dt}=-k_{r,\ L\text{-}M}[L][M]-k_{in}[P_0^{\cdot}][M]-k_p[P_r^{\cdot}][M]$
Initiator	$\frac{d[P_0X]}{dt}=-k_{r,\ I\text{-}L}[L][P_0X]-k_{r,\ I}[P_0X]+k_{d0}\left[Cu^{II}X_2\right][P_0^{\cdot}]-k_{a0}\left[Cu^IX\right][P_0X]-k_{tr,\ I}[P_r^{\cdot}][P_0X]$
Primary radical	$\frac{d[P_0^{\cdot}]}{dt}=k_{r,\ C\text{-}L}\left[Cu^{II}X_2\right][L]+2k_{r,\ I\text{-}L}[P_0X][L]+k_{r,\ MI\text{-}L}[P_rX][L]+2k_{r,\ I}[P_0X]+2k_{r,\ L\text{-}M}[L][M]-k_{in}[P_0^{\cdot}][M]+k_{a0}\left[Cu^IX\right][P_0X]-k_{d0}\left[Cu^{II}X_2\right][P_0^{\cdot}]+k_{tr,\ L}[P_r^{\cdot}][L]+k_{tr,\ I}[P_r^{\cdot}][P_0X]-2k_{t0}[P_0^{\cdot}][P_0^{\cdot}]-k_{tR}[P_r^{\cdot}][P_0^{\cdot}]$
Activator	$\frac{d[Cu^IX]}{dt}=k_{r,\ C\text{-}L}\left[Cu^{II}X_2\right][L]+k_{d0}\left[Cu^{II}X_2\right][P_0^{\cdot}]-k_{a0}\left[Cu^IX\right][P_0X]+k_d\left[Cu^{II}X_2\right][P_r^{\cdot}]-k_a\left[Cu^IX\right][P_rX]$
Deactivator	$\frac{d[Cu^{II}X_2]}{dt}=-k_{r,\ C\text{-}L}\left[Cu^{II}X_2\right][L]+k_{a0}\left[Cu^IX\right][P_0X]-k_{d0}\left[Cu^{II}X_2\right][P_0^{\cdot}]+k_a\left[Cu^IX\right][P_rX]-k_d\left[Cu^{II}X_2\right][P_r^{\cdot}]$
Ligand	$\frac{d[L]}{dt}=-k_{r,\ C\text{-}L}\left[Cu^{II}X_2\right][L]-k_{r,\ I\text{-}L}[P_0X][L]-k_{r,MI\text{-}L}[P_rX][L]-k_{r,\ L\text{-}M}[L][M]-k_{tr,\ L}[P_r^{\cdot}][L]$

the constant concentration of radicals through the reaction. However, an apparent induction period was observed before the rapid polymerization for this specific system, which might be attributed to the slow reduction of $CuBr_2$/L in response to UV light and the slow initiation of monomer by the EibBr initiator. In the case wherein original rate parameters were used, the time to complete the induction is nearly 5 h, as clearly shown in Supporting Information Figure S3A, which is longer than that observed in the experimental result. According to the mechanism shown in Table 1, the rate of the photochemical generation of radicals in the system is slower than that of the initiation reaction; thus, the light-induced reactions can be thought of as the rate-controlling steps. Therefore, the increase in photochemically mediated reaction rate can shorten the induction period.

With the idea in mind, a preliminary attempt was proposed in two steps. The four photochemical reduction rate coefficients (i.e., $k_{r,I-L}$, $k_{r,MI-L}$, $k_{r,I}$, and $k_{r,L-M}$) were derived from the model experiments with no Cu based on the steady-state approximation, and proportionated to an assumed radical termination rate coefficient (k_t).[48] Consequently, the value of k_t significantly affected the results of the derived rate coefficients. In addition, the radical termination was predominated by the termination involving small molecular radical during the reaction. In the first attempt, the values of these four rate coefficients increased to 20 times as large as the original values according to the k_t value (2.0×10^9 M^{-1} s^{-1}) used in this work, which is 20 times as large as that (1.0×10^8 M^{-1} s^{-1}) used in previous work.[48] As shown in Figure 1 (green dash-dot lines), the induction period of polymerization was shortened to approximately 2.5 h, and the conversion reached 68% after 7 h. However, the polymerization rate was still slower than the experimental result. In addition to the above four rate coefficients related to the termination rate coefficient, $k_{r,C-L}$ denotes the reduction of $CuBr_2$/L with excess ligand and derived from the semilogarithmic kinetic plot for the model experiments in the presence of Cu.[48] Herein, $k_{r,C-L}$ was considered an independent variable that can be adjusted to the experimental data. In the second step, an encouraging result showing a rapid polymerization rate and meeting the experimental results was achieved by doubling the value of $k_{r,C-L}$, as shown in Figure 1 (red lines). Notably, the induction period was further decreased (2 h), which cannot be avoided totally because of the utilization of $CuBr_2$/L and the relatively slow rate of the photochemically mediated radical generation. In addition, the chain-length dependent termination might be a factor of the deviation of simulation results from experimental data in this system at high conversion. This complicated description is usually included in the detailed models of, for example, D'hooge and Zhu et al.[1,61,63,64,69,70]

Figure 1B shows the linear evolutions of M_n with conversion for the three cases from the start of polymerization to the end. The simulation results matched well with the experimental data, although the conversions within the simulation time scale were different. The evolutions of M_w/M_n shown in Figure 1C were similar and decreased quickly after establishment of ATRP equilibrium. Addition of $CuBr_2$/L led to an inevitable induction period, but can considerably change the polymerization behavior and improve the property of the

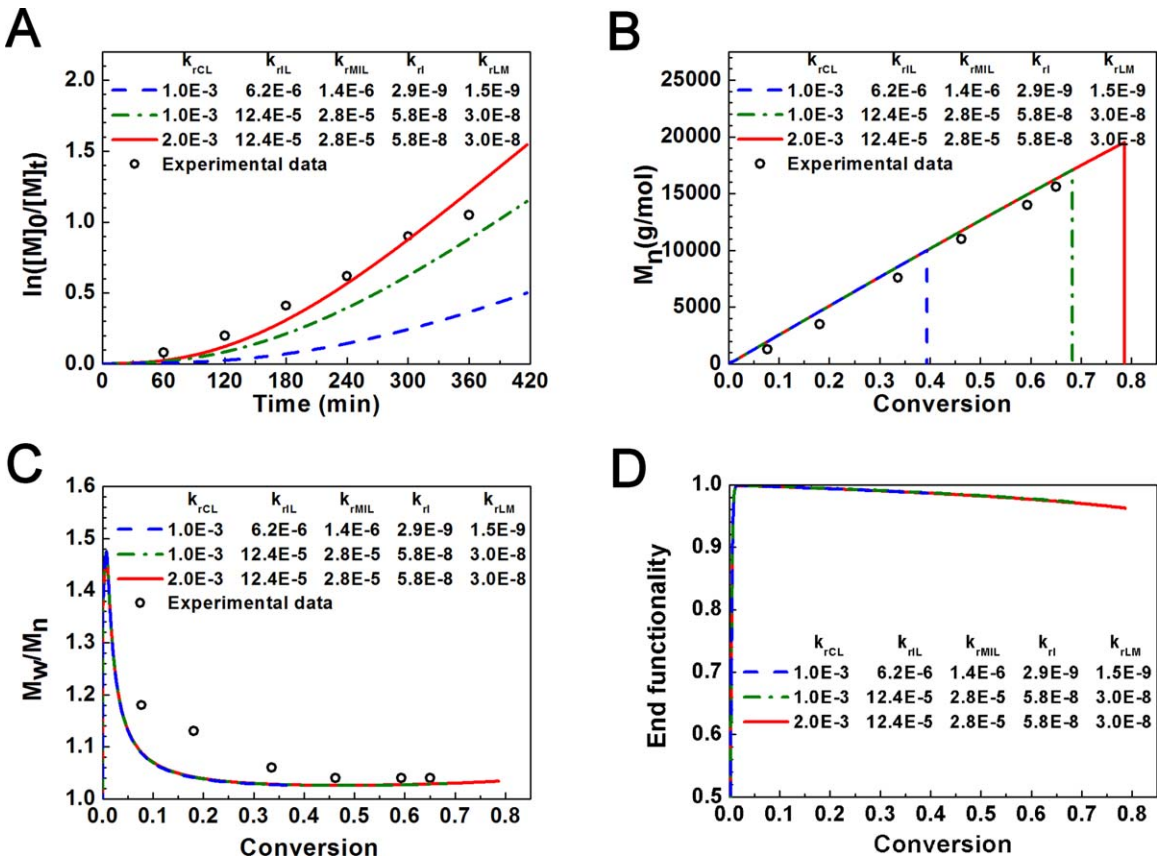

Figure 1. Comparison of the simulation results with the experimental data for photo ATRP of MA from Ref. 48: (A) semilogarithmic kinetic plot; (B) evolution of M_n with conversion; (C) evolution of M_w/M_n with conversion; (D) evolution of end functionality with conversion.

[Color figure can be viewed in the online issue, which is available at wileyonlinelibrary.com.]

resulting polymer.[24,25] On one hand, no polymer with long chain-length formed at the start of the reaction because of the sufficient deactivator that can suppress the irreversible radical termination and govern the reaction based on persistent radical effect.[71] On the other hand, the time to attain ATRP equilibrium decreased significantly compared with those of other ATRP systems that used CuBr/L as catalyst; the polydispersity index can reach as low as 1.02. The deviation between the simulation and experimental results at low conversion region is mainly caused by the adoption of ideal conditions during simulation. In addition, the test error might be another factor for this result. Figure 1D demonstrates the fraction of polymer chains with livingness. A high conversion causes the decrease of end functionality; however, the polymer chains still have high livingness (>96%) because of the mechanism of all RDRP techniques involving irreversible radical termination. Even in photo ATRP, that is only minimized. In practice, rate coefficients depend not only on reaction temperature, but also on the property of reactant. For example, radical termination rate coefficient has been described as chain-length dependence composite model.[69,70] Overall, a set of accurate rate coefficients is important for simulation, although obtaining such coefficients is a formidable task. The preliminary attempt based on a well-built kinetic model causes the simulation to meet well with practical experiment under polymerization conditions, indicating that an appropriate adjustment of photochemically mediated radical generation rate coefficients improves the fitness of simulation without disrupting the ATRP equilibrium.

Estimation of photochemically mediated radical generation rate coefficients

From the chemical engineering perspective, parameter estimation through a well-built kinetic model is a useful and efficient method, especially in situations wherein experiments cannot be carried out easily. In this study, all of the five photochemical reduction rate coefficients were estimated from the kinetic experimental data [$\ln([M]_0/[M]_t)$ vs. time] from the open report.[48] To ensure the accuracy of the resulting parameters, five sets of data at different conditions were chosen for the estimation based on least-square error calculation method. The standardized residual analysis of rate coefficients estimation is shown in Supporting Information Figure S2. In Figures 2A–C, the fitting curves describe well the characteristics of photo ATRP under specific conditions and are consistent with the experimental data, with one critical exception (black triangular symbol). The estimated kinetic parameters with the corresponding 95% confidence intervals are summarized and listed in Figure 2D. By comparison, these constants and the above adjusted parameters are in the same order of magnitude. The following kinetic investigations were carried out using the present rate parameters.

Concentration of reactants and rate of reactions for photochemically mediated ATRP

Using the developed model and estimated rate coefficients, the overall variation of the reactants and the relevant reaction

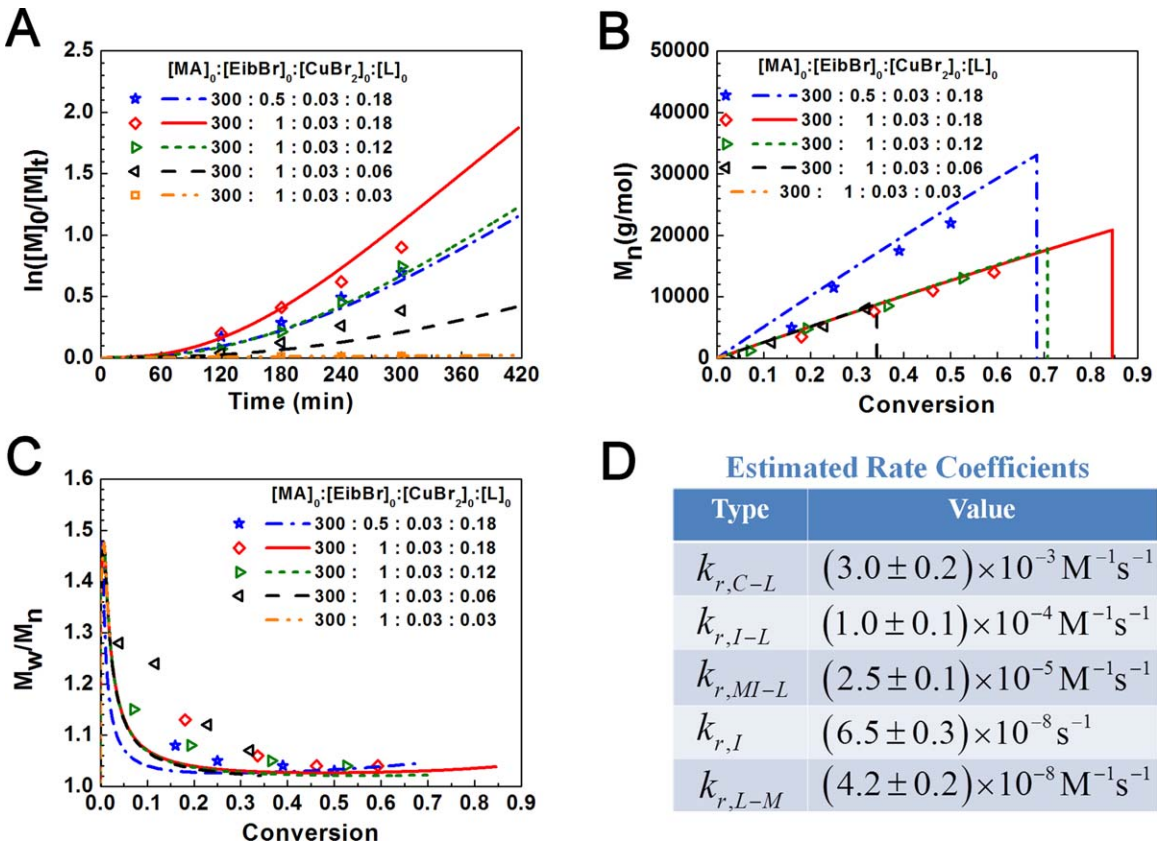

Figure 2. The corresponding fitted results for the experimental data under different conditions from Ref. 48 using the developed model: (A) semilogarithmic kinetic plot; (B) evolution of M_n with conversion; (C) evolution of M_w/M_n with conversion; (D) estimated results.

[Color figure can be viewed in the online issue, which is available at wileyonlinelibrary.com.]

rates were determined under the following conditions: $[MA]_0$:[Eib-Br]$_0$:$[CuBr_2]$:$[Me_6TREN]_0$ = 300:1:0.03:0.18, [MA] = 7.4 M, MA/DMSO = 2/1 (v/v), with 392-nm UV light irradiation at 25°C.

In response to UV light irradiation, a series of photochemically mediated radical generation reactions was triggered, as proposed in Table 1. The activator Cu(I) was generated through the reduction of deactivator Cu(II) with free L, followed by the activation of initiator (P_0X) (Figure 3A). The radical generated from the photochemical reaction and ATRP activation initiated the monomer (M) to begin the propagation [formation of growth radical species ($P_r^{\cdot}$)]. The rate of propagation (R_p) first increased and then slowed down at the end of the reaction because of the consumption of monomer, as shown in Figure 3B. However, the existence of deactivator Cu(II) can effectively deactivate both $P_0^{\cdot}$ and $P_r^{\cdot}$. Hence, it will maintain the $P_r^{\cdot}$ concentration at an extremely low level, which is typical to conventional ATRP, and leads to a small amount of P_0X residual, which is a unique trait for photo ATRP (Figure 3A). Moreover, the existence of Cu(II) can act with these continuously generated photochemical radicals (all have similar reactivity) to regenerate P_0X. With the proceeding of reaction and the establishment of ATRP equilibrium, the concentration of total radicals ($P_0^{\cdot}$ and $P_r^{\cdot}$) maintains at a low level, which leads to a small amount of P_0X residual. Another important characteristic of photo ATRP that benefited from excess Cu(II) is the rapid establishment of ATRP equilibrium, which can be clearly confirmed by the evolution of [P_rX] and the rates of activation and deactivation, as depicted in Figure 3. In general, the time to reach steady state at a constant value of [P_rX] is the transition period, which is needed to attain the ATRP equilibrium. Based on the result, the time to reach steady-state is as early as the start of polymerization. The rate of P_rX activation (R_a) overlaps that of $P_r^{\cdot}$ deactivation (R_d) nearly from the beginning to the end of the reaction, which also demonstrates that the equilibrium is established quickly. From Figure 3A, the concentration of L decreases slowly because of the relatively slow rates of the photochemical reactions ($R_{red,CL}$, $R_{red,IL}$, $R_{red,MIL}$, and $R_{red,LM}$) and transfer reaction (R_{tr}), which are commonly five to seven orders of magnitude slower than those of the ATRP reactions. Finally, given the unavoidable irreversible radical termination and chain transfer, dead polymer accumulates with the conversion, but its fraction is as low as 4.6%. As a whole, the detailed information of the photo ATRP system was vividly illustrated by the simulation, which is useful to understand the characteristics of photo ATRP.

Effect of overall photochemically mediated radical generation rate coefficients on ATRP behaviors

In this specific system, the relevant reactions regulated by UV light are the five photochemically mediated radical generation reactions. The light intensity might affect the rate coefficients of these reactions and thus affect the polymerization. Using the developed model, the simulation of photo ATRP under different overall photochemically mediated radical generation rate coefficients (k_r) was carried out and

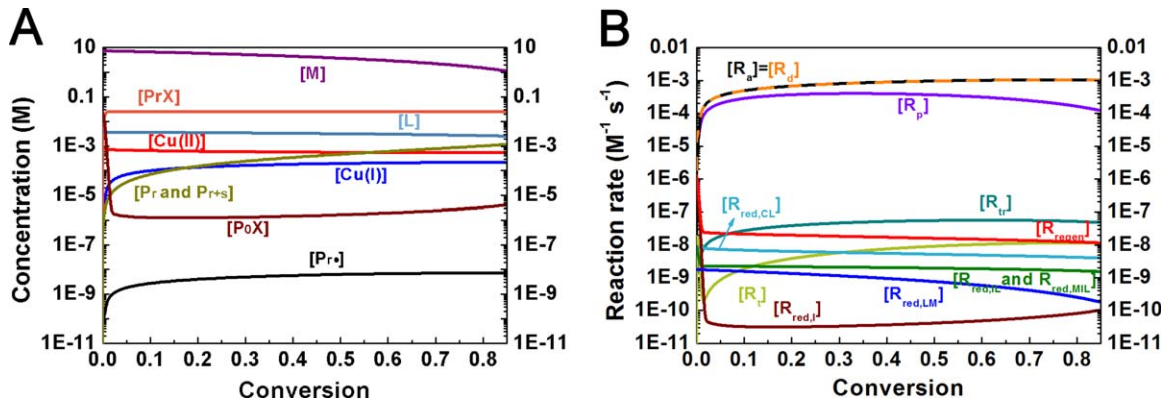

Figure 3. Reactant concentrations (A) and reaction rates (B) for photo ATRP of MA.

[Color figure can be viewed in the online issue, which is available at wileyonlinelibrary.com.]

shown in Figure 4. The conditions are the same as those used in Figure 3. The k_r value with 100% means that estimated coefficients (Figure 2D) were used and the k_r values with 50, 75, 125, and 150% mean that all five coefficients were simultaneously changed by the corresponding ratio.

From Figure 4A, the increase in k_r not only shortens the induction period but also increases the polymerization rate at steady state, which is caused by the increase of the radical generation rate. Specifically, the induction periods for different k_r values with 50, 75, 100, 125, and 150% are 168, 150, 132, 120, and 102 min, respectively. The evolution of induction time is inversely proportional to the square root of k_r magnitude, as illustrated in Supporting Information Figure S3A. The polymerization rate at steady state can be determined from the slope of the linear semilogarithmic kinetic plot (after induction period), which indicates that the concentration of the radicals in the system is constant (see Eq. 15). The plot of the apparent propagation rate coefficient (k_p^{app}) with the square root of the k_r magnitude in Supporting Information Figure S3B shows that the polymerization rate at steady state is proportional to the square root of the k_r magnitude. Actually, the square root relationship between the

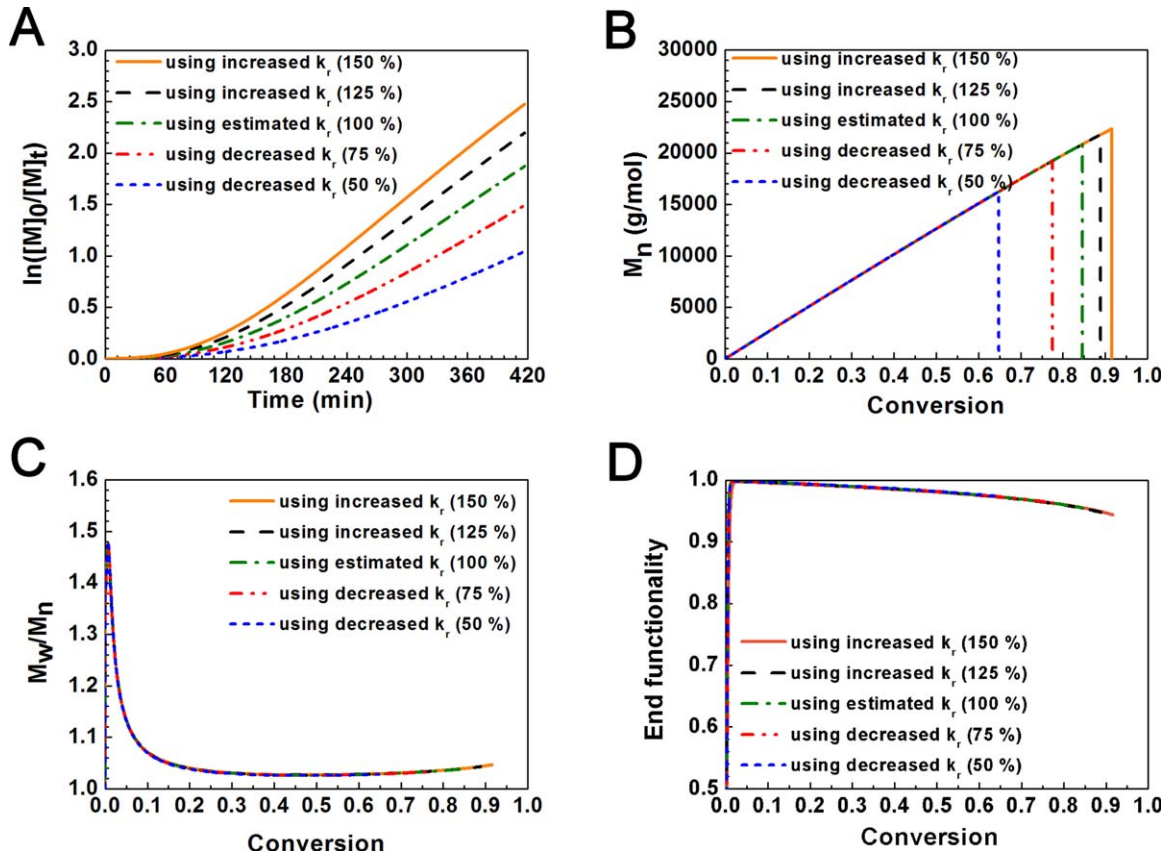

Figure 4. Simulation of photo ATRP using different overall photochemically mediated radical generation rate coefficients: (A) semilogarithmic kinetic plot; (B) evolution of M_n with conversion; (C) evolution of M_w/M_n with conversion; (D) evolution of end functionality with conversion.

[Color figure can be viewed in the online issue, which is available at wileyonlinelibrary.com.]

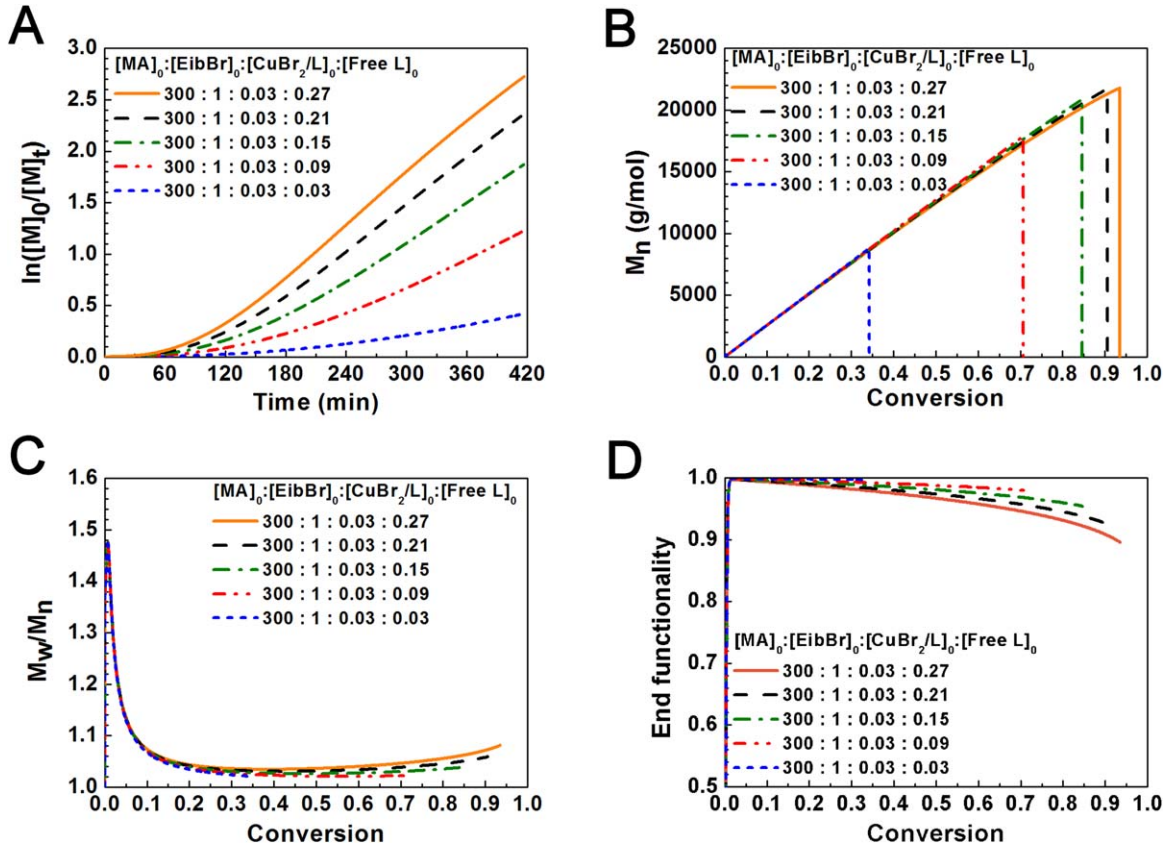

Figure 5. Simulation of photo ATRP using different free ligand concentrations: (A) semilogarithmic kinetic plot; (B) evolution of M_n with conversion; (C) evolution of M_w/M_n with conversion; (D) evolution of end functionality with conversion.

[Color figure can be viewed in the online issue, which is available at wileyonlinelibrary.com.]

reaction rate and the reaction parameters are commonly applied to other ATRP[24,25,48]

$$R_{\text{photo ATRP}} = -\frac{d[\text{M}]}{dt} = k_p[\text{P}^\cdot][\text{M}] \Rightarrow \ln\left(\frac{[\text{M}]_0}{[\text{M}]_t}\right) = k_p[\text{P}^\cdot]t = k_p^{\text{app}}t \quad (15)$$

Figures 4B, C show that the evolutions of M_n and M_w/M_n with conversion are overlapped. The linear evolution of M_n is consistent with theoretical M_n. Moreover, the evolution of M_w/M_n is lower than 1.5 at the start of polymerization and rapidly levels off to 1.04. The slight increase in M_w/M_n at high conversion might be due to the lack of monomer, and the regenerated radical can be mainly consumed through radical termination. Finally, the end functionality thus decreases to certain extent, but it is still as high as 94%. The above simulation results indicate that the change of k_r within a proper range can increase the polymerization rate without the loss of controllability.

Effect of the free ligand concentration on photo ATRP behaviors

Previous experimental studies have indicated that the free ligand concentration ([free L]$_0$) has an important role in photo ATRP system.[46,48] The most important result obtained from the two pioneer works is that the free ligand is essential for photo ATRP. No polymerization was observed through the simulation (Figure 2) at the condition that $[CuBr_2]_0$:$[L]_0$ = 1:1 (i.e., no free ligand exists in the system). Herein, the effect of the free ligand concentration on the outcome of photo ATRP was investigated by simulation, and the results were depicted in Figure 5. The simulation conditions are similar to those used in Figure 3, except the free ligand concentration.

Figure 5A indicates that the increase in free ligand concentration has a positive effect on the polymerization rate. The induction period is suppressed with the increase in polymerization rate. Supporting Information Figure S4A shows that the induction time almost linearly decreases from 270 to 90 min as [free L]$_0$ increase. In addition, the linear relationship of k_p^{app} with the square root of the free ligand concentration, which can be observed in Supporting Information Figure S4B, is consistent with the experimental results.[48] However, M_n and M_n/M_w were found to be affected by the increase in [free L]$_0$, which was ignored in the experimental study because of the experimental errors. Based on the simulation results shown in Figures 5B, C, the evolution of M_n slightly deviates from theoretical M_n at high conversion, and the polydispersity with high [free L]$_0$ is relatively higher than that with low [free L]$_0$ during polymerization. The drawbacks might be due to the generation of nonliving polymer chains, such as those initiated by small molecular radical, the transfer to ligand, and the termination by radicals. From the evolution of end functionality shown in Figure 5D, the lower the [free L]$_0$ is, the higher is the end functionality. The main reason is that increasing ligand concentration affects livingness through the transfer to ligand reaction shown in Table 1. As a whole, the investigation of the free ligand concentration indicates that the polymerization rate

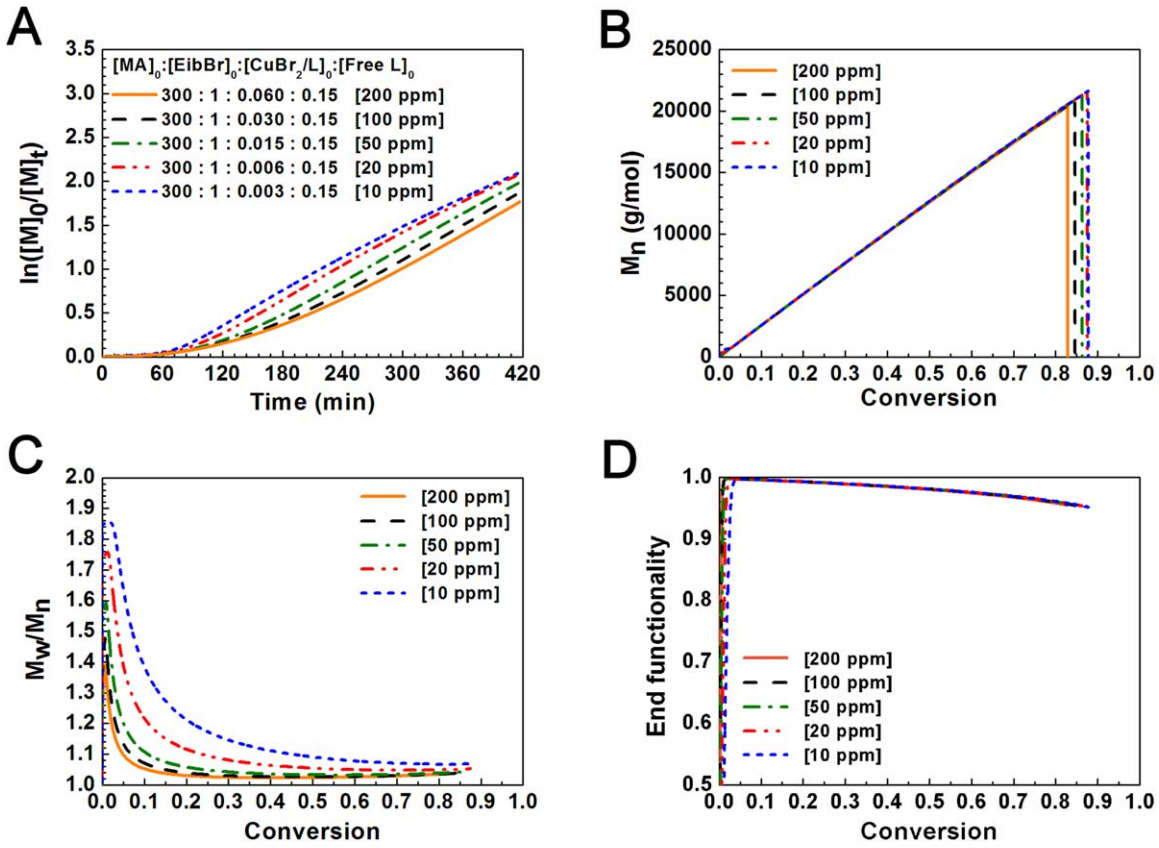

Figure 6. Simulation of photo ATRP using different catalyst concentrations: (A) semilogarithmic kinetic plot; (B) evolution of M_n with conversion; (C) evolution of M_w/M_n with conversion; (D) evolution of end functionality with conversion.

[Color figure can be viewed in the online issue, which is available at wileyonlinelibrary.com.]

can be increased by increasing the [free L]$_0$, but the controllability of the polymerization system would be slightly weakened. In addition, one can find that the polymerization rate shows the same functional response to the radical generation rate coefficients (Figure 4) and the ligand concentration (Figure 5). This can be explained as radical generation rate is proportional to the product of the above two factors (Eqs. 1–5).

Effect of the catalyst concentration on photo ATRP behaviors

The effect of catalyst concentration on ATRP system is a main concern in polymer science that needs to be addressed. Figure 6 shows the simulation results of photo ATRP using different catalyst concentrations. The simulation was performed by varying the catalyst concentration from 10 to 200 ppm with respect to the monomer concentration.

Figure 6A and Supporting Information Figure S5A demonstrate that diminishing the catalyst concentration results in the decrease of the polymerization induction time. Therefore, the corresponding conversion increases at the same reaction time (Figure 6B). However, the reaction rates reflected by the slope of the kinetic plot are nearly the same at different catalyst concentrations, as shown in Supporting Information Figure S5B. The result indicates that the polymerization rate does not depend on the catalyst concentration, which is similar to the conventional ATRP without deactivator, but different from the other ATRP systems with deactivator, such as ICAR ATRP and ARGET ATRP. Generally, the absolute amount of catalyst (commonly Cu species) in ATRP can be decreased under normal ATRP conditions without affecting the rate of polymerization, which is ultimately governed by a ratio of the concentrations of Cu(I) to Cu(II) species.[12] However, the unavoidable irreversible radical termination and the accumulation of persistent radical [Cu(II) deactivator] in practical polymerization system leads to about 1–10% loss of polymeric end functionality, unless there is larger enough catalyst concentration (commonly $>$ 1000 ppm).[12] It is well known that a decrease in deactivator concentration causes an increase in the polymerization rate of ICAR ATRP[14] but slows down the reaction rate of ARGET ATRP.[19] For the former one, the activator is continuously generated from the activation of the deactivator by conventional initiator radical. If the amount of the initial deactivator is too low, the propagating radical would not be effectively deactivated by the deactivator, thereby accelerating of the polymerization rate and increasing polydispersity index at the early stage of polymerization. For the latter one, the activator is gradually generated from the reduction of the deactivator by excess reducing agent. The higher the deactivator loading is, the higher is the amount of the activator. Therefore, the polymerization rate speeds up, and the controllability of polymerization is improved. Based on the results in this system, the independence of k_p^{app} on the initial catalyst concentration, (Figure 6A and Supporting Information Figure S5B), the higher polydispersity index at low conversion (Figure 6C), and the loss of end functionality (Figure 6D) might be the consequences of the synergistic effect of ARGET ATRP and ICAR ATRP. In this regard, the reduction

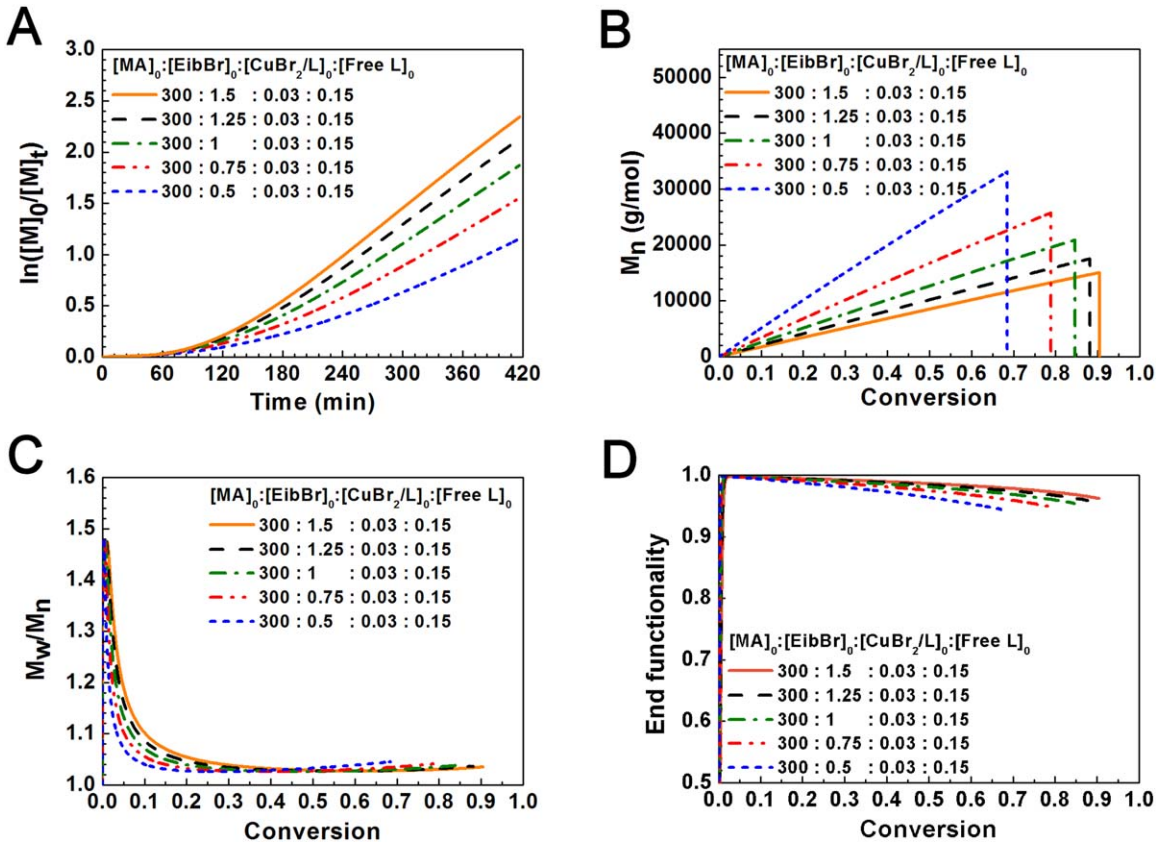

Figure 7. Simulation of photo ATRP using different initiator concentrations: (A) semilogarithmic kinetic plot; (B) evolution of M_n with conversion; (C) evolution of M_w/M_n with conversion; (D) evolution of end functionality with conversion.

[Color figure can be viewed in the online issue, which is available at wileyonlinelibrary.com.]

of $CuBr_2$/L in the presence of excess ligand through UV light stimuli resembles the ARGET ATRP process, and the photochemical SET reaction between either Eib-Br or PMA-Br with excess ligand is similar to ICAR ATRP process. Herein, a bold but rational speculation is proposed that the mechanism of photo ATRP is a combination of ARGET ATRP and ICAR ATRP, which coincides with the result obtained in a previous work.[48]

Effect of the initiator concentration on photo ATRP behaviors

A simulation was conducted to study the kinetic behaviors of photo ATRP under different initial initiator concentration. Figure 7 shows that the initiator concentration has a significant effect on the polymerization kinetics.

As depicted in Figure 7A, the induction time is shortened and the reaction rate speeds up as the initiator concentration increases. Interestingly, a linear relationship between k_p^{app} and the square root of the initiator concentration was also observed in Supporting Information Figure S6B. In terms of this acceleration, the increase in $[EibBr]_0$ (shorter targeted chain-length) causes the high radical concentration by shifting the ATRP equilibrium, and thus increases the polymerization rate, which is the same as that in ICAR ATRP and ARGET ATRP processes.[15,16,72] In addition, the photochemical reactions that involve the initiator might also contribute to this speed up. However, the relationship between the polymerization rate and initiator concentration is to the half power, which is an interesting point in this specific system as theoretically derived in Ribelli et al.'s work.[48] Figure 7B shows that the evolution of M_n with conversion matches the theoretical M_n well, and the long polymer chain-length is as expected because of the low $[EibBr]_0$. The development of M_w/M_n in Figure 7C also indicates that low initiator concentration helps establish the ATRP equilibrium. This can be explained as a lower $[EibBr]_0$ usually implies a faster ATRP initiation, which is helpful for instantaneously propagation.[16] Based on the evolution of end functionality, the result wherein low $[EibBr]_0$ with low radical concentration can lead to the decrease in end functionality seems impossible. According to Eq. 14, the decrease in F_t is mainly due to the low dormant species concentration, which is a determinant in the denominator (in the system, the concentration of the radical species or dead polymer species is extremely low). The above simulation results illustrate that the characteristics of photo ATRP under different initiator concentrations are similar to but not the same as those of ATRP processes with low initial Cu loading.

Conclusion

To sum up, a case study of the kinetics of photochemically mediated ATRP was carried out based on a newly clarified mechanism through simulation approach. A comprehensive kinetic model was developed using the method of

moments, which is not only used to study the polymerization behaviors but also to estimate the uncertain reaction rate coefficients.

In this specific case, the photochemically mediated radical generation rate coefficients were first adjusted to the experimental data through the trial and error method. The as-developed model was then used to estimate five coefficients. The results indicate that the original coefficients derived from the experiments are lower than the adjusted or estimated results and thus cause the simulation results to deviate from the experimental data. The evolution of reactants and the rates of each reaction in photo ATRP system show the unique characteristics of photo ATRP, such as rapid ATRP equilibrium and quick consumption of small initiator with a small amount of residual.

Simulations on the effects of overall photochemically mediated radical generation rate coefficients (k_r), as well as that of the concentrations of the free ligand, catalyst, and initiator on ATRP behaviors were also investigated. The results show that the acceleration of polymerization rate can be achieved by increasing the k_r, the free ligand concentration, or the initiator concentration. The development of k_p^{app} with the square root of these three parameters is linear, which is a typical law followed by other ATRP processes. However, the independence of k_p^{app} on the square root of [$CuBr_2$/L] was observed in this work. These results indicate that the mechanism of photo ATRP is a combination of ARGET ATRP and ICAR ATRP.

Overall, through the kinetic modeling (old method) of photo ATRP (new mechanism), the underlying mechanism and the optimization of polymerization condition were demonstrated in detail.

Acknowledgment

The authors thank the National Natural Science Foundation of China (No. 21276213), the Research Fund for the Doctoral Program of Higher Education (No. 20130073110077), and the National High Technology Research and Development Program of China (No. 2013AA032302) for supporting this work.

Literature Cited

1. Zhu S, Hamielec A. Polymerization kinetic modeling and macromolecular reaction engineering. In: Matyjaszewski K, Möller M, editors. *Polymer Science: A Comprehensive Reference, Vol.* 4. Amsterdam: Elsevier BV, 2012:779–831.
2. Fogler HS. Elements of Chemical Reaction Engineering, 4th ed. Upper Saddle River, New Jersey: Prentice Hall, 2005.
3. Smith JM. *Chemical Engineering Kinetics*, 3rd ed. New Delhi: McGraw Hill, 1981.
4. Braunecker WA, Matyjaszewski K. Controlled/living radical polymerization: features, developments, and perspectives. *Prog Polym Sci*. 2007;32:93–146.
5. Jenkins AD, Jones RG, Moad G. Terminology for reversible-deactivation radical polymerization previously called "controlled" radical or "living" radical polymerization. *Pure Appl Chem*. 2010; 82:483–491.
6. Matyjaszewski K. Atom transfer radical polymerization (ATRP): current status and future perspectives. *Macromolecules*. 2012;45: 4015–4039.
7. Matyjaszewski K, Tsarevsky NV. Nanostructured functional materials prepared by atom transfer radical polymerization. *Nat Chem*. 2009;1:276–288.
8. Matyjaszewski K, Tsarevsky NV. Macromolecular engineering by atom transfer radical polymerization. *J Am Chem Soc*. 2014;136: 6513–6533.
9. Destarac M. Controlled radical polymerization: industrial stakes, obstacles and achievements. *Macromol React Eng*. 2010;4:165–179.
10. Chan N, Cunningham MF, Hutchinson RA. Reducing ATRP catalyst concentration in batch, semibatch and continuous reactors. *Macromol React Eng*. 2010;4:369–380.
11. Chan N, Cunningham MF, Hutchinson RA. Copper-mediated controlled radical polymerization in continuous flow processes: synergy between polymer reaction engineering and innovative chemistry. *J Polym Sci Part A: Polym Chem*. 2013;51:3081–3096.
12. Matyjaszewski K, Jakubowski W, Min K, Tang W, Huang J, Braunecker WA, Tsarevsky NV. Diminishing catalyst concentration in atom transfer radical polymerization with reducing agents. *Proc Natl Acad Sci USA*. 2006;103:15309–15314.
13. Konkolewicz D, Magenau AJD, Averick SE, Simakova A, He H, Matyjaszewski K. ICAR ATRP with ppm Cu catalyst in water. *Macromolecules*. 2012;45:4461–4468.
14. D'hooge DR, Konkolewicz D, Reyniers M-F, Marin GB, Matyjaszewski K. Kinetic modeling of ICAR ATRP. *Macromol Theory Simul*. 2012;21:52–69.
15. Toloza Porras C, D'hooge DR, Reyniers M-F, Marin GB. Computer-aided optimization of conditions for fast and controlled ICAR ATRP of n-butyl acrylate. *Macromol Theory Simul*. 2013;22:136–149.
16. Toloza Porras C, D'hooge DR, Van Steenberge PHM, Reyniers M-F, Marin GB. ICAR ATRP for estimation of intrinsic macro-activation/deactivation arrhenius parameters under polymerization conditions. *Ind Eng Chem Res*. 2014;53:9674–9685.
17. Jakubowski W, Matyjaszewski K. Activators regenerated by electron transfer for atom-transfer radical polymerization of (meth)acrylates and related block copolymers. *Angew Chem Int Ed*. 2006;45:4482–4486.
18. Li X, Wang W-J, Li B-G, Zhu S. Kinetics and modeling of solution ARGET ATRP of styrene, butyl acrylate, and methyl methacrylate. *Macromol React Eng*. 2011;5:467–478.
19. Payne KA, D'hooge DR, Van Steenberge PHM, Reyniers M-F, Cunningham MF, Hutchinson RA, Marin GB. ARGET ATRP of butyl methacrylate-utilizing kinetic modeling to understand experimental trends. *Macromolecules*. 2013;46:3828–3840.
20. Zhang N, Samanta SR, Rosen BM, Percec V. Single electron transfer in radical ion and radical-mediated organic, materials and polymer synthesis. *Chem Rev*. 2014;114:5848–5958.
21. Monteiro MJ, Guliashvili T, Percec V. Kinetic simulation of single electron transfer-living radical polymerization of methyl acrylate at 25°C. *J Polym Sci Part A: Polym Chem*. 2007;45:1835–1847.
22. Haehnel AP, Fleischmann S, Hesse P, Hungenberg K-D, Barner-Kowollik C. Investigating Cu(0)-mediated polymerizations new kinetic insights based on a comparison of kinetic modeling with experimental data. *Macromol React Eng*. 2013;7:8–23.
23. Konkolewicz D, Wang Y, Zhong M, Krys P, Isse AA, Gennaro A, Matyjaszewski K. Reversible-deactivation radical polymerization in the presence of metallic copper. A critical assessment of the SARA ATRP and SET-LRP Mechanisms. *Macromolecules*. 2013;46:8749–8772.
24. Zhong M, Wang Y, Krys P, Konkolewicz D, Matyjaszewski K. Reversible-deactivation radical polymerization in the presence of metallic copper. *Kinetic simulation. Macromolecules*. 2013;46:3816–3827.
25. Zhou Y-N, Luo Z-H. Copper(0)-mediated reversible-deactivation radical polymerization: kinetics insight and experimental study. *Macromolecules*. 2014;47:6218–6229.
26. Magenau AJD, Strandwitz NC, Gennaro A, Matyjaszewski K. Electrochemically mediated atom transfer radical polymerization. *Science*. 2011;332:81–84.
27. Dadashi-Silab S, Tasdelen MA, Yagci Y. Photoinitiated atom transfer radical polymerization: current status and future perspectives. *J Polym Sci Part A: Polym Chem*. 2014;52:2878–2888.
28. Yamago S, Nakamura Y. Recent progress in the use of photoirradiation in living radical polymerization. *Polymer*. 2013;54:981–994.
29. Alfredo NV, Jalapa NE, Morales SL, Ryabov AD, Le Lagadec R, Alexandrova L. Light-driven living-controlled radical polymerization of hydrophobic monomers catalyzed by ruthenium(II) metalacycles. *Macromolecules*. 2012;45:8135–8146.
30. Ohtsuki A, Goto A, Kaji H. Visible-light-induced reversible complexation mediated living radical polymerization of methacrylates with organic catalysts. *Macromolecules*. 2013;46:96–102.
31. Fors BP, Hawker CJ. Control of a living radical polymerization of methacrylates by light. *Angew Chem Int Ed*. 2012;51:8850–8853.
32. Treat NJ, Fors BP, Kramer JW, Christianson M, Chiu C-Y, de Alaniz JR, Hawker CJ. Controlled radical polymerization of acrylates regulated by visible light. *ACS Macro Lett*. 2014;3:580–584.

33. Xu J, Jung K, Atme A, Shanmugam S, Boyer C. A robust and versatile photoinduced living polymerization of conjugated and unconjugated monomers and its oxygen tolerance. *J Am Chem Soc*. 2014; 136:5508–5519.
34. Xu J, Jung K, Boyer C. Oxygen tolerance study of photoinduced electron transfer-reversible addition-fragmentation chain transfer (PET-RAFT) polymerization mediated by $Ru(bpy)_3Cl2$. *Macromolecules*. 2014;47:4217–4229.
35. Shanmugam S, Xu J, Boyer C. Photoinduced electron transfer-reversible addition-fragmentation chain transfer (PET-RAFT) polymerization of vinyl acetate and N-vinylpyrrolidinone: kinetic and oxygen tolerance study. *Macromolecules*. 2014;47:4930–4942.
36. Treat NJ, Sprafke H, Kramer JW, Clark PG, Barton BE, Read de Alaniz J, Fors BP, Hawker CJ. Metal-free atom transfer radical polymerization. *J Am Chem Soc*. 2014;136:16096–16101.
37. Miyake GM, Theriot JC. Perylene as an organic photocatalyst for the radical polymerization of functionalized vinyl monomers through oxidative quenching with alkyl bromides and visible light. *Macromolecules*. 2014;47:8255–8261.
38. Telitel S, Dumur F, Telitel S, Soppera O, Lepeltier M, Guillaneuf Y, Poly J, Morlet-Savary F, Fioux P, Fouassierd J-P, Gigmes D, Lalevee J. Photoredox catalysis using a new iridium complex as an efficient toolbox for radical, cationic and controlled polymerizations under soft blue to green lights. *Polym Chem*. 2015;6:613–624.
39. Guan Z, Smart B. A remarkable visible light effect on atom-transfer radical polymerization. *Macromolecules*. 2000;33:6904–6906.
40. Kwak Y, Matyjaszewski K. Photoirradiated atom transfer radical polymerization with an alkyl dithiocarbamate at ambient temperature. *Macromolecules*. 2010;43:5180–5183.
41. Tasdelen MA, Uygun M, Yagci Y. Photoinduced controlled radical polymerization. *Macromol Rapid Commun*. 2011;32:58–62.
42. Tasdelen MA, Uygun M, Yagci Y. Photoinduced controlled radical polymerization in methanol. *Macromol Chem Phys*. 2010;211:2271–2275.
43. Ciftci M, Tasdelen MA, Li W, Matyjaszewski K, Yagci Y. Photoinitiated ATRP in inverse microemulsion. *Macromolecules*. 2013;46: 9537–9543.
44. Mosnáček J, Ilčíková M. Photochemically mediated atom transfer radical polymerization of methyl methacrylate using ppm amounts of catalyst. *Macromolecules*. 2012;45:5859–5865.
45. Konkolewicz D, Schröder K, Buback J, Bernhard S, Matyjaszewski K. Visible light and sunlight photoinduced ATRP with ppm of Cu catalyst. *ACS Macro Lett*. 2012;1:1219–1223.
46. Anastasaki A, Nikolaou V, Zhang Q, Burns J, Samanta SR, Waldron C, Haddleton AJ, McHale R, Fox D, Percec V, Wilson P, Haddleton DM. Copper(II)/tertiary amine synergy in photoinduced living radical polymerization: accelerated synthesis of ω-functional and α,ω-heterofunctional poly(acrylates). *J Am Chem Soc*. 2014;136:1141–1149.
47. Anastasaki A, Nikolaou V, Simula A, Godfrey J, Li M, Nurumbetov G, Wilson P, Haddleton DM. Expanding the scope of the photoinduced living radical polymerization of acrylates in the presence of $CuBr_2$ and Me_6-Tren. *Macromolecules*. 2014;47:3852–3859.
48. Ribelli TG, Konkolewicz D, Bernhard S, Matyjaszewski K. How are radicals (re)generated in photochemical ATRP? *J Am Chem Soc*. 2014;136:13303–13312.
49. Ribelli TG, Konkolewicz D, Pan X, Matyjaszewski K. Contribution of photochemistry to activator regeneration in ATRP. *Macromolecules*. 2014;47:6316–6321.
50. Zhang T, Chen T, Amin I, Jordan R. ATRP with a light switch: photoinduced ATRP using a household fluorescent lamp. *Polym Chem*. 2014;5:4790–4796.
51. Chuang Y-M, Ethirajan A, Junkers T. Photoinduced sequence-controlled copper-mediated polymerization: synthesis of decablock copolymers. *ACS Macro Lett*. 2014;3:732–737.
52. Anastasaki A, Nikolaou V, Pappas GS, Zhang Q, Wan C, Wilson P, Davis TP, Whittaker MR, Haddleton DM. Photoinduced sequence-control via one pot living radical polymerization of acrylates. *Chem Sci*. 2014;5:3536–3542.
53. Tang W, Kwak Y, Braunecker W, Tsarevsky NV, Coote ML, Matyjaszewski K. Understanding atom transfer radical polymerization: effect of ligand and initiator structures on the equilibrium constants. *J Am Chem Soc*. 2008;130:10702–10713.
54. Buback M, Kurz CH, Schmaltz C. Pressure dependence of propagation rate coefficients in free-radical homopolymerizations of methyl acrylate and dodecyl acrylate. *Macromol Chem Phys*. 1998;199: 1721–1727.
55. Fischer H, Radom L. Factors controlling the addition of carbon-centered radicals to alkenes-an experimental and theoretical perspective. *Angew Chem Int Ed*. 2001;40:1340–1371.
56. Wang Y, Soerensen N, Zhong M, Schroeder H, Buback M, Matyjaszewski K. Improving the "livingness" of ATRP by reducing Cu catalyst concentration. *Macromolecules*. 2013;46:683–691.
57. Bamford CH, Dyson RW, Eastmond GC. Network formation IV. The nature of the termination reaction in free-radical polymerization. *Polymer*. 1969;10:885–899.
58. Johnston-Hall G, Monteiro MJ. Bimolecular radical termination: new perspectives and insights. *J Polym Sci Part A: Polym Chem*. 2008; 46:3155–3173.
59. Barner-Kowollik C, Beuermann S, Buback M, Castignolles P, Charleux B, Coote ML, Hutchinson RA, Junkers T, Lacik I, Russell GT, Stachj M, van Herklm AM. Critically evaluated rate coefficients in radical polymerization-7. Secondary-radical propagation rate coefficients for methyl acrylate in the bulk. *Polym Chem*. 2014;5:204–212.
60. Zhu S. Modeling of molecular weight development in atom transfer radical polymerization. *Macromol Theory Simul*. 1999;8:29−37.
61. Delgadillo-Velazquez O, Vivaldo-Lima E, Quintero-Ortega IA, Zhu S. Effects of diffusion-controlled reactions on atom-transfer radical polymerization. *AIChE J*. 2002;48:2597−2608.
62. Wang R, Luo YW, Li BG, Zhu S. Control of gradient copolymer composition in ATRP using semibatch feeding policy. *AIChE J*. 2007;53:174–186.
63. D'Hooge DR, Reyniers M-F, Marin GB. Methodology for kinetic modeling of atom transfer radical polymerization. *Macromol React Eng*. 2009;3:185−209.
64. D'hooge DR, Reyniers M-F, Stadler FJ, Dervaux B, Bailly C, Du Prez FE, Marin GB. Atom transfer radical polymerization of isobornyl acrylate: a kinetic modeling study. *Macromolecules*. 2010;43: 8766−8781.
65. Zhou Y-N, Li J-J, Luo Z-H. Synthesis of gradient copolymers with simultaneously tailor-made chain composition distribution and glass transition temperature by semibatch ATRP. *J Polym Sci Part A: Polym Chem*. 2012;50:3052−3066.
66. Zhou Y-N, Luo Z-H, Chen JH. Theoretical modeling coupled with experimental study on the preparation and characterization comparison of fluorinated copolymers: effect of chain structure on copolymer properties. *AIChE J*. 2013;59:3019–3033.
67. Zhou Y-N, Luo Z-H. Insight into the ATRP rate controlling ability of initiator structure: micromolecular, macromolecular, and immobilized initiators. *J Polym Sci Part A: Polym Chem*. 2014;52:2228−2238.
68. Wang W, Zhou Y-N, Luo Z-H. Modeling of the atom transfer radical copolymerization processes of methyl methacrylate and 2-(trimethylsilyl) ethyl methacrylate under batch, semibatch, and continuous feeding. *Ind Eng Chem Res*. 2014;53:11873–11883.
69. Vana P, Davis TP, Barner-Kowollik C. Easy access to chain-length-dependent termination rate coefficients using RAFT polymerization. *Macromol Rapid Commun*. 2002;23:952–956.
70. Derboven P, D'hooge DR, Reyniers M-F, Marin GB, Barner-Kowollik C. The long and the short of radical polymerization. *Macromolecules*. 2015;48:492–501.
71. Fischer H. The persistent radical effect: a principle for selective radical reactions and living radical polymerizations. *Chem Rev*. 2001; 101:3581–3610.
72. Simakova A, Averick SE, Konkolewicz D, Matyjaszewski K. Aqueous ARGET ATRP. *Macromolecules*. 2012;45:6371–6379.

Manuscript received Jan. 11, 2015, and revision received Feb. 27, 2015.